

# Silylcarborane Acrylate Nanoimprint Lithography Resists

Yoan C. Simon,<sup>†</sup> Isaac W. Moran,<sup>†</sup> Kenneth R. Carter,\* and E. Bryan Coughlin\*

Department of Polymer Science and Engineering, University of Massachusetts, Amherst, Massachusetts 01003

**ABSTRACT** The synthesis of a novel silylcarborane acrylate monomer is reported as well as its application as an etch-resistant component for the formulation of imprint layers for UV nanoimprint lithography (NIL). By introduction of 10% by weight of the silylcarborane acrylate monomer into NIL resist formulations, the oxygen plasma etch rate of the resulting film was reduced by nearly a factor of 2. When used in NIL, the patterned resist layer had excellent oxygen plasma etch resistance, leading to effective image transfer to the underlying poly(hydroxyethyl methacrylate) lift-off layer. The latter allowed for the fabrication of metallic interdigitated electrode patterns via a NIL/lift-off process. This work demonstrates the robustness of silylcarborane-containing resists and paves the way for the investigation of new, high-resolution patterning methods.

**KEYWORDS:** carboranes • nanoimprint lithography • hybrid materials • etch resistance • lift-off

## INTRODUCTION

Carboranes, and more specifically icosahedral carboranes, have been utilized in various areas of research, including boron neutron capture therapy (1–3), nonlinear optical materials, and superacid chemistry (4, 5). Recently, carborane-containing polymers have shown promising results in a variety of nanotechnological applications (6) and, more specifically, in lithographic systems (7–9). For instance, Ober has synthesized boron-containing polymeric resists for extreme UV lithography starting with poly(styrene-*b*-1,2-butadiene) copolymers followed by a postpolymerization functionalization approach employing the pendant olefins and a hydroboration/hydroxylation procedure to attach pendant carborane cages (7). The advantage of tethering inorganic clusters to a polymeric matrix is that both the processability of polymers and the etch resistance of inorganics are combined within a single material. The resistance of inorganic clusters stems from the potential of forming nonvolatile oxides upon treatment with an oxygen plasma etch. Boron clusters are particularly interesting from the standpoint of generating novel resists because of their transparency to UV, and particularly extreme UV (10).

With applications ranging from microelectronics to protein nanoarrays (11, 12), nanoimprint lithography (NIL) is a very useful technique whose domain of utilization is continuously expanding thanks to its ease of implementation and high-throughput capability (13). NIL is intriguing from a cost perspective because imprint systems do not require the sophisticated optics of conventional steppers. Rather, imprint lithography uses polymers that harden while conforming to a physical template upon exposure to UV light

or upon a thermal transition. In particular, UV-NIL limits pattern distortion and accelerates the patterning process (14). It is therefore a particularly attractive nanopatterning method. As UV-NIL grows into a widespread patterning technique, the composition of UV-cross-linkable resists becomes accordingly more and more diversified and sophisticated. One can draw similarities among the formulations used in conventional photoresists (15). These comprise a series of monomers, for polymerization (monofunctional), cross-linking, and etch resistance, as well as a UV-sensitive free-radical initiator. All of these components are dissolved in a suitable solvent to allow for spin-casting. Additionally, the viscosity of the ensemble is controlled to permit low-temperature embossing.

One of the most critical material components in the imprint lithographic process is the photopolymerized resist layer; sometimes this resist layer is called the etch barrier or imaging layer. The resist polymer chemistry needs to be designed so that it provides higher etch resistance (selectivity) than the underlying layer, which allows for pattern transfer. While NIL resists that contain no inorganic additives have been used to make patterned magnetic media with features as small as 35 nm, the performance is limited by the innate material properties of the resist layer (16). Several advances have been made to improve the properties of resists for NIL. One of the challenges associated with the fabrication of metalized features at the nanoscale resides in the fabrication of overhang structures that are convenient for the lift-off step. Matsui et al. have elegantly addressed the issue of lift-off by utilizing water-soluble poly(vinyl alcohol) as the replicated material (17). This method is all the more interesting because it opens new perspectives in terms of “green chemistry”. However, such a technique requires the use of thermal NIL, which could eventually pose problems for the replication of small features in addition to the associated costs. Willson et al. have shown more recently a method whereby the imprinted resist could be un-cross-

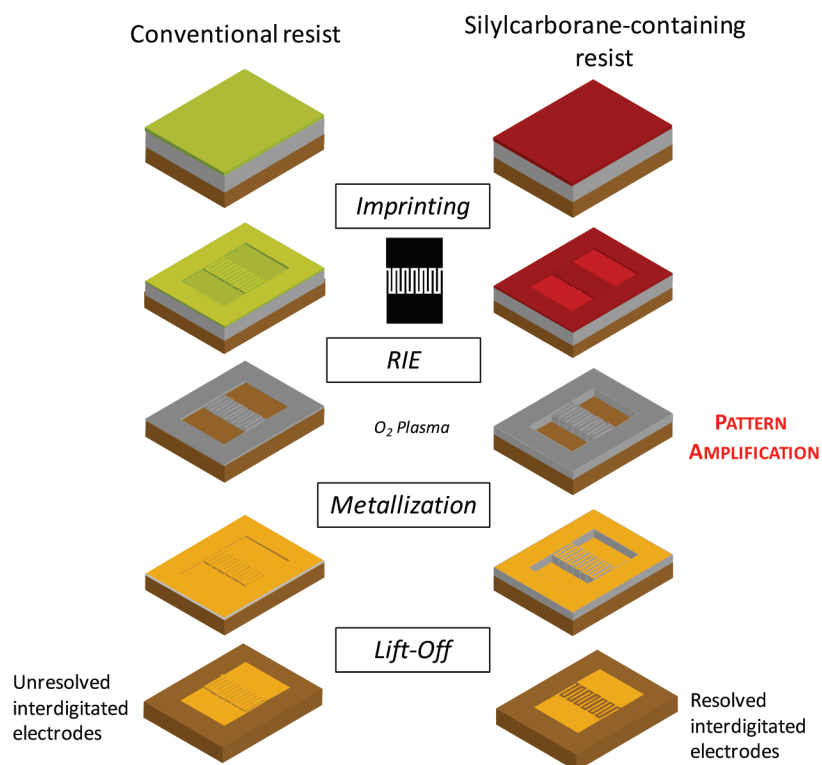
\* E-mail: Coughlin@mail.pse.umass.edu (E.B.C.), Carter@polysci.umass.edu (K.R.C.).

Received for review April 3, 2009 and accepted July 29, 2009

<sup>†</sup> Both of these authors contributed equally.

DOI: 10.1021/am900229z

© 2009 American Chemical Society

Scheme 1. Comparative Schematic Illustrating the Mechanism by Which the Patterns Are Obtained<sup>a</sup>

<sup>a</sup> The brown layer represents the silicon wafer, the gray layer is the imprint layer, and the top layers are the two respective types of formulations.

linked to allow for facile stripping of the copolymer network constituting the resist (15). Moran et al. have demonstrated an improved nanoimprint lithographic process involving precuring using a commercial polyurethane resist that was used to make transistor devices after lift-off (16).

The introduction of inorganic materials into resists has been a common route for increasing oxygen plasma etch resistance. For example, the Willson group employs siloxane-containing acrylate monomers in their NIL resist formulations (14). Carter et al. recently reported the use of phosphazene-containing monomers in UV-NIL formulations, leading to excellent etch resistance properties (18).

Lift-off is a particular concern when the mask features are shallow (19). In order to obtain high-fidelity pattern transfer across a substrate regardless of its roughness, it is preferable to convert shallow imprints into higher-aspect-ratio resist stacks. This is achieved in UV-NIL through enhanced contrast between the etch rates of the cross-linked imprint resist and the soluble underlayer. Therefore, it is essential to design and formulate imprint resists that will provide sufficient etch resistance to allow for pattern amplification (Scheme 1). Increased feature depth facilitates lift-off, and therefore pattern transfer, by allowing the solvents to penetrate below the metalated features. This is critical for the broader implementation of NIL.

In this report, the synthesis of a well-defined acrylate monomer containing both boron and silicon and its incorporation into UV-NIL resists is described. The resistance to oxygen plasma etching is compared to a conventional resist formulation. We then take advantage of the increased etch resistance of silyl-functionalized carboranes to generate a

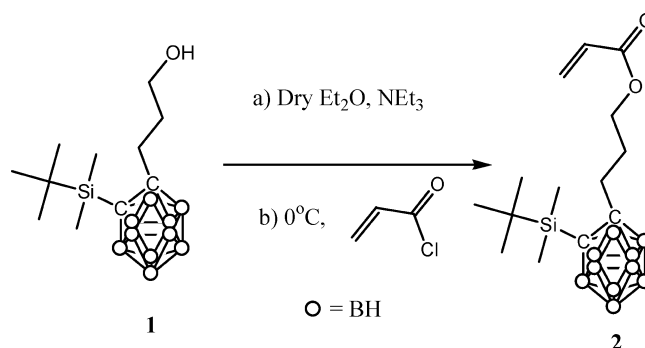


FIGURE 1. Synthesis of 2.

significant etch contrast with the underlayer and enable the fabrication of high-aspect-ratio features. Microscopy combined with profilometry was utilized to demonstrate pattern amplification. The patterns were subsequently metalized, and the lift-off step was shown to be improved by the presence of boron and silicon in the resist formulation.

## RESULTS AND DISCUSSION

We focused on the development of a novel type of etch-resistant monomer to facilitate the lift-off process in the case of shallow patterns, allowing for the fabrication of cleaner metalated structures by NIL. The synthesis of silylcarborane acrylate (2) is depicted in Figure 1. Two of us recently described an optimized preparation of 1 that was based on a previous synthesis published by Gomez and Hawthorne (20). The incorporation of a silyl group on the carborane serves a dual purpose. In the first case, the steric demands of this group ensure the monosubstitution of *ortho* carbo-

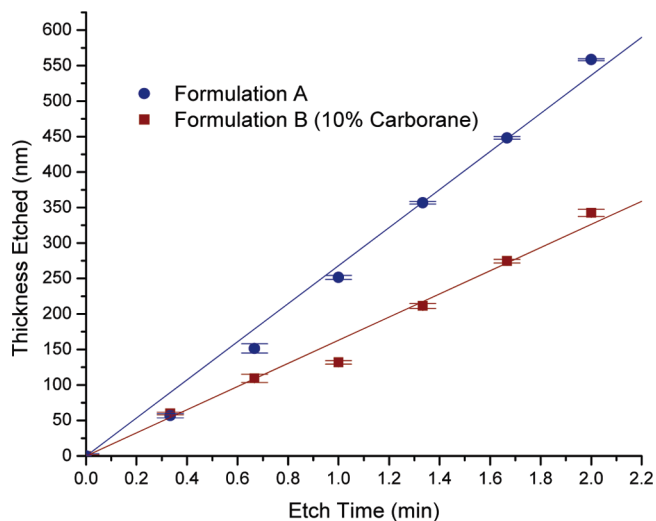


FIGURE 2. Determination of the etch rates of the control formulation A and the modified B resists.

rane, allowing for the high-yield preparation of **1**. Additionally, the presence of silicon will contribute to the reinforcement of the overall etch resistance of the material by adding one more element capable of forming a stable nonvolatile oxide upon oxygen plasma treatment. The slow dropwise addition of acryloyl chloride to a cooled solution of **1** in dry diethyl ether, in the presence of a slight excess of a scavenger base ( $\text{NEt}_3$ ), results in the formation of **2** and the concomitant production of triethylammonium chloride. Following a standard liquid–liquid extraction procedure and recrystallization from hexanes, **2** was obtained in good yield as a colorless solid.

To evaluate the etch resistance enhancement provided by the incorporation of monomer **2**, two solutions of UV-curable, multifunctional acrylate monomers were spun-cast from propylene glycol methyl ethyl acetate (PGMEA) onto silicon wafers, cured under a UV lamp, and etched using oxygen plasma. The first formulation (A) was a conventional resist used for UV-NIL and served as a control (see Experimental Methods). The second formulation (B) was prepared by taking formulation A and adding 10% by weight of the carborane acrylate **2**. This concentration of **2** was selected because it offered a clear demonstration of the influence on etch resistance at a reasonable level of incorporation. Figure 2 illustrates the difference in the etch rate between the control formulation A and the carborane-containing counterpart formulation B. Assuming that both UV-cured materials are homogeneous along the direction perpendicular to the wafer and that the etch rates of both materials are linear with respect to the etching time, etch rates of approximately 268 nm/min for A and 163 nm/min for B were obtained. These results were obtained by averaging the thicknesses measured by spectral reflectance of 10 spots per cured sample.

Once the enhanced etch resistance was established, imprints were performed with the two formulations onto PHEMA-coated silicon wafers. The purpose of the PHEMA film was 3-fold. First, it provided adhesion between the UV-NIL resist and the silicon substrate upon being coated with

Table 1. Imprint and Etch Profilometry Results

sample	imprint depth (nm)	etch depth (nm)	height change (nm)	amp. factor <sup>a</sup>
A	55.4	63.6	8.2	1.15
B	56.9	131.0	74.1	2.30

<sup>a</sup> Amplification factor = etch depth/imprint depth.

an adhesion promoter. Second, it served as an orthogonally soluble underlayer to provide lift-off after subsequent metallization. Third, it provided a standard etch contrast to the UV-NIL formulations A and B. Table 1 contains the profilometry measurements for imprinted and subsequently etched features. Given that the same mask was utilized for imprints in A and B, it is understandable that the corresponding imprint depths are equivalent, and this finding suggests that the incorporation of **2** does not introduce any noticeable change in the imprint process parameters. However, the drastic difference in the feature depth after etching, here referred to as the etch depth, confirms the possibility of amplifying features by means of the incorporation of **2**. The amplification factor corresponds to the difference in the etch rate between the PHEMA underlayer and the UV-NIL resist formulation. In the case of formulation A, the etch rates of the resist and underlayer are relatively similar because the final feature height upon breakthrough is only 10 nm deeper than that of the imprint. However, there is a clear difference in etch rates when formulation B is utilized, which results in more than a 2-fold increase in the feature height upon breakthrough.

Two patterns, small and large interdigitated electrodes, were imprinted onto the resists to demonstrate visually the difference in the depth amplification. The patterns were imprinted and etched using an oxygen plasma reactive ion etch (RIE). Micrometric features were chosen so as to facilitate the characterization of the imprints, and all images are taken at the point of breakthrough to the underlying wafer during RIE. In the case of imprints realized with the conventional formulation A (Figure 3i,iii), a brown film can be observed, indicating that the film covering the surface is relatively thin, below 100 nm. In contrast, a thicker blue film was observed at breakthrough when **2** is incorporated (Figure 3ii,iv). This coloration is an additional qualitative confirmation of the efficacy of **2** to act as an etch-resistant additive.

This difference in the resist thickness at breakthrough is critical as far as allowing the patterns to be used successfully in a lithographic process. The patterns were coated with gold by vacuum evaporation, and a lift-off step was performed using methanol. After metallization and lift-off, it can be clearly seen that the thicknesses of the features prepared using formulation A were not tall enough to allow easy diffusion of the lift-off solvent under the interdigitated features (Figure 4 and Scheme 1). However, in the case of the amplified features prepared by means of incorporating the carborane-modified resist B, the lift-off easily resolves the interdigitated lines.

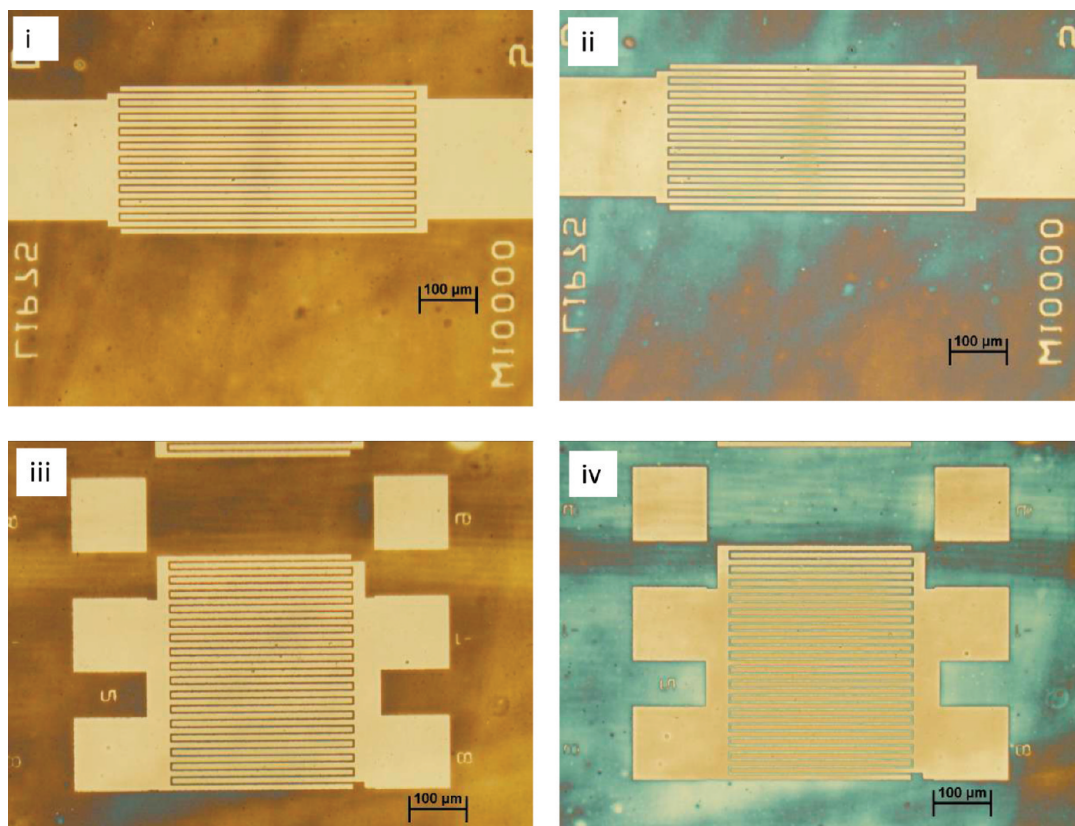


FIGURE 3. Imprinted and etched device features. On the left are features patterned into unmodified formulation A (i and iii), and on the right are the same features patterned into formulation B (ii and iv).

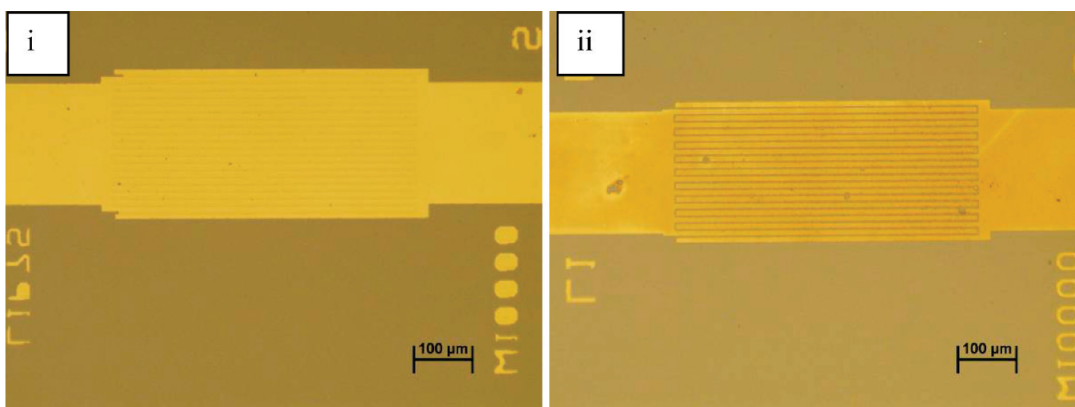


FIGURE 4. Patterned gold features: (i) unresolved interdigitated electrodes using formulation A as an imprint layer (left) and (ii) resolved patterns observed using the B resist (right).

## CONCLUSION

A novel acrylate monomer **2** containing an inorganic boron cluster that is further functionalized with a silicon-containing group has been synthesized. The incorporation of 10% by weight of **2** in the formulation for UV-NIL showed a significant improvement in the etch resistance of the imprint layer. Additionally, the etch rates measured using an oxygen plasma were considerably decreased relative to a control sample lacking both boron and silicon and lead to an amplification improvement of a factor of 2. The latter contributed to facilitating the lift-off step after metallization of interdigitated electrode patterns. The utilization of inorganic cluster additives in resist technology is a novel approach to the application of features in UV-NIL, and we are

currently investigating the possibility of expanding this methodology to other types of inorganic cluster additives.

## EXPERIMENTAL METHODS

**General Materials.** All solvents and reagents were obtained from Aldrich and VWR and were used without further purification unless specified otherwise. Single-sided, polished, mechanical-grade, 1.5-in. silicon wafers were purchased from University Wafer. Ethoxylated bisphenol A dimethacrylate from Sartomer, methanol and chlorodimethyloctylsilane (97%) from Fisher, 2-ethyl-2-(hydroxymethyl)-1,3-propanediol triacrylate, 2,2-dimethoxy-2-phenylacetophenone, 2-hydroxyethyl methacrylate (HEMA; 98%),  $\alpha,\alpha'$ -azoisobutyronitrile (AIBN; 98%), 1-dodecanethiol (98%), 3-(trimethoxysilyl)propyl methacrylate (98%), and propylene glycol methyl ether acetate (PGMEA) from Sigma-Aldrich, gold (99.999%; Kurt J. Lesker), and chromium (R. D.

Mathis) were used as received. Silylcarboranylpropanol (**1**) was prepared as previously described (20, 21).

**Instrumentation.**  $^1\text{H}$  and  $^{13}\text{C}$  NMR were recorded at 300 MHz and 128 and 100 MHz, respectively, on a Bruker NMR spectrometer at room temperature in deuterated chloroform. The individual NMR spectral assignments do not list the carborane B–H resonances. Because of the quadrupolar nature of boron, the resonances for the 10 B–H bonds are observed as broad multiplets [ $\delta$  (ppm) = 3.20–1.01]. The integration of these multiplets accounts for 10 hydrogen atoms. Gel permeation chromatography (GPC) measurements for the lift-off layer polymer were performed in tetrahydrofuran (THF) at 1.0 mL/min using a Knauer K-501 pump, with a K-2301 refractive index detector and a K-2600 UV detector, and a column bank consisting of two Polymer Laboratories PLGel Mixed D columns at 40 °C. All other measurements were performed using a similar system with a column bank consisting of three Polymer Laboratories PLGel Mixed D columns at 40 °C. Molecular weights are reported relative to polystyrene standards.

**Silicon Master Templates.** Silicon wafers containing test patterns were fabricated by known photolithographic processes. Interdigitated transistor structures of 60 nm depth and various length/width ratios with critical dimensions down to 3  $\mu\text{m}$  were patterned over a 4.0  $\text{cm}^2$  wafer chip. The silicon masters were prepared for photopolymer mold (PP-mold) casting by exposure to  $\text{O}_2$  plasma for 3 min, coating with neat chlorodimethyloctylsilane, and heating to 130 °C for 20 min to create a protective alkyl release layer to ensure the proper separation of cured PP-molds.

**Photopolymer Formulation A.** Ethoxylated bisphenol A dimethacrylate (76.5 wt %), 2-ethyl-2-(hydroxymethyl)-1,3-propanediol triacrylate (23.2 wt %), and 2,2-dimethoxy-2-phenylacetophenone (2.5 wt %) as initiators were combined in an opaque vial and diluted with PGMEA to 10 wt % overall.

**Photopolymer Formulation B.** Formulation A (90 wt %) and silylcarborane acrylate (**2**; 10 wt %) were combined in an opaque vial and diluted with PGMEA to 10 wt % overall.

**Synthesis of **2**.** In a dry round-bottomed flask, **1** (1 equiv) was dissolved in freshly distilled ether. The solution was placed under a nitrogen flow with constant agitation, and triethylamine (1.5 equiv) was added dropwise with a syringe. The mixture was cooled to 0 °C, and acryloyl chloride (1.3 equiv) was added dropwise to the solution. Upon addition, a white precipitate formed, indicating formation of the triethylammonium salt. The mixture was then allowed to warm to room temperature and stirred for 1 h. A solution of saturated brine was then added, and the organic and aqueous phases were separated in a separatory funnel flask. The aqueous phase was further extracted with 2  $\times$  50 mL of diethyl ether. The organic phases were combined and dried over  $\text{MgSO}_4$  and concentrated in vacuo to afford a yellowish powder. The powder was then dissolved in boiling hexanes and recrystallized at –4 °C (yield = 73 %). Mp: 117 °C.  $^1\text{H}$  NMR ( $\text{CDCl}_3$ , 400 MHz):  $\delta$  6.40 (q, 1H,  $J_{\text{trans}} = 16$  Hz,  $J_{\text{gem}} = 1.6$  Hz), 6.07 (q, 1H,  $J_{\text{cis}} = 9.2$  Hz,  $J_{\text{trans}} = 16$  Hz), 5.85 (q, 1H,  $J_{\text{gem}} = 1.6$  Hz,  $J_{\text{cis}} = 9.2$  Hz), 4.14 (t, 2H,  $\text{CH}_2\text{O}$ ), 3.20–1.01 (br, 10H, BH,  $\text{CH}_2$ ,  $\text{CH}_2\text{CB}$ ), 1.05 (s, 9H,  $\text{SiCH}_3$ ), 0.26 (s, 6H,  $\text{CCH}_3$ ).  $^{13}\text{C}$  NMR ( $\text{CDCl}_3$ ):  $\delta$  165.93, 131.35, 127.96, 80.51, 76.25, 63.13, 34.73, 29.38, 27.59, 20.35, –2.49. HRMS (FAB). Calcd for  $\text{C}_{14}\text{H}_{35}\text{B}_{10}\text{O}_2\text{Si}$ :  $m/z$  371.3418. Found:  $m/z$  371.3469.

**Synthesis of Poly(hydroxyethyl methacrylate) (PHEMA).** Ethanol (7.5 mL) was charged in a 25 mL round-bottomed flask, and nitrogen was bubbled for 5 min. AIBN (0.07 g, 0.43 mmol), HEMA (5.37 g, 5 mL, 41.31 mmol), and dodecanethiol (0.43 g, 0.5 mL) were dissolved in ethanol, the flask was sealed with a rubber stopper, and the solution was heated under nitrogen at 60 °C for 4 h with stirring. The solution was cooled and precipitated dropwise into hexanes. The polymer was filtered,

washed with hexanes, and dried to obtain PHEMA (4.5 g, 84 %) as a white solid. GPC data (in DMF):  $M_n = 32\,000$  g/mol, PDI = 1.37.

**PP-Mold Preparation.** Square glass coverslips of #2 thickness, 4.8  $\text{cm}^2$  in area, from Fisher were rinsed with acetone and isopropyl alcohol and dried under a stream of nitrogen. The surface of the glass was then activated by exposure to 100 mTorr oxygen plasma at 30 W for 7 min. Immediately after activation, the glass pieces were immersed in a dry, nitrogen-purged toluene solution containing [3-(methacryloxy)propyl]-trimethoxysilane (1% v/v) and heated at 80 °C for 12 h to assemble an adhesion monolayer. Polymeric relief structures were formed on the treated glass by placing a small drop (~50  $\mu\text{L}$ ) of formulation A photocurable acrylate resin on the silicon master and carefully laying a piece of treated glass over the drop, allowing capillary forces to spread the resin between the two surfaces. The two pieces were then exposed to 365 nm UV light to cure the resin. Careful separation of the two surfaces yielded nanopatterned features bonded to the glass slide. A release layer was applied over the cured polymer features to aid separation during the contact-molding process.

**Contact Molding with an Etch Resist.** Silicon substrates were cleaned by rinsing with THF, acetone, and isopropyl alcohol and blown dry with a stream of nitrogen. PHEMA (6.5 wt % in methanol) was applied to the substrate and spun at 3000 rpm for 10 s, followed by baking at 130 °C for 30 s, forming a 180-nm-thick PHEMA film. An adhesion promoter, 3-(trimethoxysilyl)propyl methacrylate, was then applied and spun at 3000 rpm for 5 s, and the sample was baked at 130 °C for 1 min. Excess adhesion promoter was washed off by spinning under a pure stream of PGMEA for 15 s at 3000 rpm, followed by drying with nitrogen. Photopolymer by itself or loaded with 10 wt % carboraneacrylate, diluted in PGMEA to 10 wt % overall (viscosity approximately 5 cps), and filtered through a 0.45  $\mu\text{m}$  syringe filter was then applied and spun at 3000 rpm for 15 s, yielding a 137-nm-thick film.

Immediately after spin coating, a PP-mold was placed directly on the photopolymer film and the setup was inserted into the NX-2000 imprinter. After pressurization to 75 psi, the photopolymer was cured by 365 nm UV light (25 mW/cm<sup>2</sup>) for 30 s. Release of the sample from the PP-mold yielded patterned substrates. The resist undergoes a 3% volume contraction during curing, which helps to facilitate release from the imprint mold.

**Etching, Metal Deposit, and Lift-Off Step.** Patterned films were etched in a Trion Technologies Phantom III inductively couple plasma (ICP) reactive ion etcher under 250 mTorr of oxygen pressure at a flow rate of 49 sccms, with ICP and RIE power of 500 and 25 W, respectively, until the underlying silicon wafer was exposed in the recessed regions throughout the imprint (~80 s for photopolymer and ~105 s for photopolymer/CBER). Etched wafers were coated with approximately 2 nm of chromium, followed by 10 nm of gold by vacuum evaporation. Lift-off was achieved by sonication in warm methanol for 5–10 min, followed by a methanol rinse.

**Acknowledgment.** The authors acknowledge financial support from the NSF (NSF Career Award DMR-0239475 to E.B.C.). A sabbatical fellowship from the Max Planck Gesellschaft to E.B.C. and the hospitality and facilities provided by the Max Planck Institute for Polymer Research in Mainz, Germany, are also gratefully acknowledged. This research was also kindly supported by the UMass Center for Hierarchical Manufacturing, a NSF Nanoscale Science and Engineering Center (Grant DMI-0531171).

## REFERENCES AND NOTES

- (1) Hawthorne, M. F. *Angew. Chem., Int. Ed. Engl.* **1993**, *32*, 950–984.
- (2) Parrott, M. C.; Marchington, E. B.; Valliant, J. F.; Adronov, A. J. *Am. Chem. Soc.* **2005**, *127* (34), 12081–12089.
- (3) Valliant, J. F.; Guenther, K. J.; King, A. S.; Morel, P.; Schaffer, P.; Sogbein, O. O.; Stephenson, K. A. *Coord. Chem. Rev.* **2002**, *232* (1–2), 173–230.
- (4) Murphy, D. M.; Mingos, D. M. P.; Forward, J. M. *J. Mater. Chem.* **1993**, *3* (1), 67–76.
- (5) Reed, C. A. *Chem. Commun.* **2005**, (13), 1669–1677.
- (6) Malenfant, P. R. L.; Wan, J.; Taylor, S. T.; Manoharan, M. *Nat. Nanotechnol.* **2007**, *2* (1), 43–46.
- (7) Dai, J.; Ober, C. K. *Proc. SPIE—Int. Soc. Opt. Eng.* **2003**, *5039* (Advances in Resist Technology and Processing XX), 1164–1171.
- (8) Dai, J.; Ober, C. K. *Proc. SPIE—Int. Soc. Opt. Eng.* **2004**, *5376* (Part 1, Advances in Resist Technology and Processing XXI), 508–516.
- (9) Dai, J.; Ober, C. K.; Wang, L.; Cerrina, F.; Nealey, P. *Proc. SPIE—Int. Soc. Opt. Eng.* **2002**, *4690* (Advances in Resist Technology and Processing XIX), 1193–1202.
- (10) Bratton, D.; Yang, D.; Dai, J. Y.; Ober, C. K. *Polym. Adv. Technol.* **2006**, *17* (2), 94–103.
- (11) Gates, B. D.; Xu, Q. B.; Stewart, M.; Ryan, D.; Willson, C. G.; Whitesides, G. M. *Chem. Rev.* **2005**, *105* (4), 1171–1196.
- (12) Guo, L. J. *J. Phys. D: Appl. Phys.* **2004**, *37* (11), R123–R141.
- (13) Krauss, P. R.; Chou, S. Y. *Appl. Phys. Lett.* **1997**, *71* (21), 3174–3176.
- (14) Stewart, M. D.; Willson, C. G. *MRS Bull.* **2005**, *30* (12), 947–951.
- (15) Palmieri, F.; Adams, J.; Long, B.; Heath, W.; Tsiartas, P.; Willson, C. G. *ACS Nano* **2007**, *1* (4), 307–312.
- (16) Moran, I. W.; Briseno, A. L.; Loser, S.; Carter, K. R. *Chem. Mater.* **2008**, *20*, 4595–4601.
- (17) Nakamatsu, K.; Tone, K.; Matsui, S. *Jpn. J. Appl. Phys. Part 1* **2005**, *44* (11), 8186–8188.
- (18) Hagberg, E. C.; Hart, M. W.; Cong, L. H.; Allen, C. W.; Carter, K. R. *J. Inorg. Organomet. Polym. Mater.* **2007**, *17* (2), 377–385.
- (19) Guo, L. J. *Adv. Mater.* **2007**, *19* (4), 495–513.
- (20) Simon, Y. C.; Ohm, C.; Zimny, M. J.; Coughlin, E. B. *Macromolecules* **2007**, *40* (16), 5628–5630.
- (21) Gomez, F. A.; Hawthorne, M. F. *J. Org. Chem.* **1992**, *57* (5), 1384–1390.

AM9002292